Model discrimination for drying and rehydration kinetics of freeze-dried tomatoes

Lopez-Quiroga, Estefania; Prosapio, Valentina; Fryer, Peter; Norton, Ian; Bakalis, Serafim

DOI:
10.1111/jfpe.13192

Document Version
Publisher's PDF, also known as Version of record

Citation for published version (Harvard):
Lopez-Quiroga, E, Prosapio, V, Fryer, P, Norton, I & Bakalis, S 2019, 'Model discrimination for drying and rehydration kinetics of freeze-dried tomatoes', *Journal of Food Process Engineering*. https://doi.org/10.1111/jfpe.13192

Received: 15 March 2019 | Revised: 25 June 2019 | Accepted: 30 June 2019

DOI: 10.1111/jfpe.13192

ORIGINAL ARTICLE

Journal of Food Process Engineering WILEY

Model discrimination for drying and rehydration kinetics of freeze-dried tomatoes

Estefania Lopez-Quiroga[1] | Valentina Prosapio[1] | Peter J. Fryer[1] | Ian T. Norton[1] | Serafim Bakalis[1,2]

[1]School of Chemical Engineering, University of Birmingham, Birmingham, United Kingdom

[2]Faculty of Engineering, University of Nottingham, Nottingham, United Kingdom

Correspondence
Valentina Prosapio, School of Chemical Engineering, University of Birmingham, Birmingham B15 2TT, United Kingdom.
Email: v.prosapio@bham.ac.uk

Funding information
Engineering and Physical Sciences Research Council, Grant/Award Numbers: EP/K011820/1, EP/K030957/1

Abstract

The aim of this work is to investigate the effect of a highly interconnected porous microstructure on the quality of rehydrated tomatoes by (a) designing a freeze-dried cycle that ensure product integrity (i.e., no collapse, no puffing) (b) characterizing both freeze-drying and rehydration kinetics. Fresh tomatoes were first freeze-dried and subsequently rehydrated to get generate kinetics data. Afterwards, six thin-layer drying models and four rehydration models were fitted using regression analysis to the experimental data. The goodness-of-fit was evaluated according to root mean squared error, adjusted R^2, Akaike information criterion, and Bayesian information criterion. The most accurate representations of the system kinetics were observed using the Page model for freeze-drying and the exponential and Weibull models for rehydration. Rehydration capacities and equilibrium moisture contents of the rehydrated samples were found to increase with temperature, and the corresponding activation energy values were calculated.

Practical applications

Freeze-dried porous microstructures can enhance water absorption and transport, contributing to restore the fresh product functional properties and leading to higher quality rehydrated products, especially in highly heat-sensitive food products as vegetables and fruits. The use of mathematical models to (a) design freeze-drying cycles and (b) characterize and/or predict drying and rehydration kinetics in cellular freeze-dried microstructures is then key for processing and optimization of convenience and ready-to-eat foods, which represents the main application of dried foods/powders and also a growing market. This approach to the manufacture of freeze-dried products also presents potential to set the basis of an alternative decentralized supply scenario for high-quality dried products, where freeze-dried foods will be manufactured and shipped and finally rehydrated closer to the consumption point.

1 | INTRODUCTION

Among the different drying processes employed in the food industry, freeze-drying is considered the best technique to produce high-quality dried products (Andrieu & Vessot, 2018; Ratti, 2001; Sagar & Suresh Kumar, 2010). During freeze-drying operations, the product is first frozen and the formed ice is then removed by sublimation at pressures close to vacuum (Qiao, Fang, Huang, & Zhang, 2013), causing

negligible structure damage (Alfat & Purqon, 2017; Ratti, 2001). Freeze-drying typically creates a porous microstructure characterized by interconnected networks, which results in shorter rehydration times and higher rehydration capacities than in products dried using any other method (Lewicki, Le, & Pomarańska-Łazuka, 2002; Lewicki & Wiczkowska, 2006; Meda & Ratti, 2005; Omolola, Jideani, & Kapila, 2017).

Ladha-Sabur et al. (Ladha-Sabur, Bakalis, Fryer, & Lopez-Quiroga, 2019) reviewed the energy demands of food manufacturing processes. From an industrial point of view, freeze-drying is both expensive and high-energy consuming (Karam, Petit, Zimmer, Baudelaire Djantou, & Scher, 2016; Lopez-Quiroga, Antelo, & Alonso, 2012; Tarafdar, Shahi, Singh, & Sirohi, 2018). As foods consist mostly of water, phase changes involved during freeze-drying (i.e., solidification, sublimation, and vaporization/condensation) represent the main contribution to the total process energy demand (Lopez-Quiroga, Wang, Gouseti, Fryer, & Bakalis, 2016). However, energy consumption—and thus environmental impact during processing—can be reduced either by optimal process design (Bosca, Barresi, & Fissore, 2016; Lopez-Quiroga et al., 2012) or by combination with other drying techniques (Prosapio, Norton, & De Marco, 2017; Zhang, Chen, Mujumdar, Zhong, & Sun, 2015). Moreover, the reduced weight of dried products can also contribute to decrease the total environmental burden, making transportation more efficient than if the products are transported in a nondry state.

Generally, freeze-dried products are rehydrated prior to their use to recover the properties of the fresh product (Krokida & Philippopoulos, 2005; Prosapio & Norton, 2017, 2018). In this framework, a distributed manufacturing model could represent an interesting alternative (Baldea, Edgar, Stanley, & Kiss, 2017; Roos et al., 2016). In this model, only valuable ingredients are shipped and any other additive or component (such as water) can be added later at the local level. Processing plants would thus create freeze-dried foodstuff and convey it to a local and smaller network formed by multiple rehydration points closer to the consumer. This would result in a more energy efficient scenario that would also satisfy consumers demand for more sustainable products (see, e.g., the cost calculations of Almena, Fryer, Bakalis, and Lopez-Quiroga [2019]). Ensuring a fast rehydration and the preservation of the food organoleptic properties thus becomes critical to the design, development, and optimization of freeze-dried convenience and ready-to-eat foods. The rehydration ability of the food depends from the microstructural damage experienced during the drying process (Krokida & Marinos-Kouris, 2003; Marques, Prado, & Freire, 2009). For example, in plant cells—that is, fruits and vegetables, which are highly heat-sensitive—over drying of the product may lead to the loss of the cell turgor and collapse of the food structure (Joardder, Kumar, & Karim, 2017), preventing the dried product regaining its initial moisture content (A. Marabi & Saguy, 2004; Marques et al., 2009). Due to the low processing temperatures – that also minimize the loss of flavor compounds and nutrients—freeze-drying has found a wide field of application in fruits and vegetables processing (Bourdoux, Li, Rajkovic, Devlieghere, & Uyttendaele, 2016; Karathanos, Anglea, & Karel, 1996; Khalloufi & Ratti, 2003; Marabi & Saguy, 2004; Meda & Ratti, 2005).

Dehydration kinetics are typically modeled by fitting the experimental drying curves to (a) empirical thin-layer models (e.g., Wang and Singh, Weibull), (b) semitheoretical ones derived from Newton's (e.g., Lewis, Page, and modified Page) or Fick's second laws (e.g., exponential, two-term, logarithmic, and Henderson and Pabis), and (c) first-order kinetics models (C. Ertekin & Firat, 2017; Krokida & Philippopoulos, 2005; Onwude, Hashim, Janius, Nawi, & Abdan, 2016). Often, the fitted drying constants are employed to estimate moisture diffusivities and activation energies of the drying process (Sampaio et al., 2017; Vega-Gálvez et al., 2015). Complexity of models arises as the number of parameters involved grows: for example, the Newton model involves a single parameter, whereas the modified Henderson and Pabis use six constants (Onwude et al., 2016). Few studies have addressed modeling of freeze-drying kinetics independently and most commonly they are studied in comparison with other drying techniques (Colucci, Fissore, Mulet, & Cárcel, 2017; Krokida & Marinos-Kouris, 2003; Link, Tribuzi, & Laurindo, 2017; Onwude et al., 2016). A similar approach is followed to model rehydration kinetics of freeze-dried fruits and vegetables. Studies have focused on the effect of different drying methods and temperature of the rehydration medium (water) on the restitution capacity of the dried product, making use of both empirical models (e.g., Peleg and Weibull) and theoretical expressions (e.g., capillarity and first-order kinetics) to describe water uptake kinetics (Gaware, Sutar, & Thorat, 2010; Krokida & Philippopoulos, 2005). In this case again, rehydration models are assessed in terms of their goodness-of-fit without considering complexity (i.e., number of constants involved).

The production of fresh tomatoes in 2014 was about 17 Mt in EU and 70 Mt worldwide (FAO, 2014). Despite their relevance on the global market, studies focused on freeze-drying/rehydration of this fruit are scarce in literature and show a limited modeling approach, involving few kinetic models and/or absence of model discrimination. Another relevant aspect that published studies on freeze-dried tomatoes tend to ignore is the effect of freeze-drying conditions on the microstructure of the tomatoes and how this can affect subsequent rehydration processes (and kinetics). For example, Krokida and Philippopoulos (2005) used a single model (i.e., first-order kinetic law) to analyze the rehydration kinetics of tomatoes (among other vegetables) at different temperatures, and they analyzed different quality parameters (density, texture, flavor, etc.) upon rehydration; no details on the freeze-drying process were provided in this work, although they did point out that shrinkage caused during drying can prevent rehydration. Chawla, Kaur, Oberoi, and Sogi (2008) used a single thin-layer model (unique model) to compare freeze-drying kinetics of tomato pulp to other drying configurations (cabinet, tray, and fluidized bed) and determined sorption isotherms, but they did not undertake the study of rehydration kinetics nor evaluated the structure of the tomatoes before and after processing (drying). Gaware et al. (2010) also studied freeze-drying of tomatoes in comparison to other drying techniques (hot-air, solar, heat-pump, and microwave vacuum drying), and they performed rehydration experiments at two different

temperatures (25 and 100°C). However, they used only Page's model to describe freeze-drying kinetics (without reporting initial and final microstructure of the samples) and Peleg's model to analyzed rehydration kinetics (but without reporting any significant effect of temperature on the process).

To fill the gap between freeze-drying processing conditions, dried microstructure and rehydration performance, this work presents a comprehensive study of both drying and rehydration kinetics of freeze-dried tomatoes through combined experimental and modeling approaches. Freeze-drying experiments were designed and implemented taking into account the specific composition and thermal/mass transfer properties of tomatoes—that is, bounds for the operational temperatures at different chamber pressures were determined by identifying the corresponding glass transition (T'_g) and collapse (T_{col}) temperatures—which ensured structural integrity of the samples by avoiding shrinkage and/or collapse. To describe the system kinetics, six thin-layer drying models (Newton, Page, Henderson and Pabis, logarithmic, two-term, and Wang and Singh) and four rehydration models (Peleg, exponential, first-order, and Weibull) were considered, which enable model discrimination analysis: information theory methods (Akaike information criterion [AIC] and Bayesian information criteria [BIC]) were used to discriminate the models by their accuracy and the number of parameters involved, identifying those that better described the system kinetics. Those models were then employed to investigate the system kinetics, with special attention to the analysis of rehydration capacities and kinetics as a function of the medium temperature. This allowed the characterization of the governing rehydration mechanism and the calculation of the corresponding activation energies.

2 | MATERIALS AND METHODS

2.1 | Materials

Fresh tomatoes were purchased in a local supermarket and stored in a refrigerator at 5°C. After washing, draining with blotting paper, and removing the external impurities, the tomato pericarp was cut into pieces of 1 cm × 1 cm × 2 cm (height × width × length).

2.2 | Moisture content analysis

Moisture content analyses were carried out using a moisture analyzer (model MB 25, OHAUS, Switzerland). Two gram of fresh sample was placed in the analyzer and uniformly heated at 120°C until the sample weight became constant. The moisture percentage as a function of weight change was then recorded. Tomato initial moisture content was found to be equal to 92.3 ± 1.21% w/w.

2.3 | Freeze-drying experiments

Fresh samples were frozen at −20°C and then dried under vacuum (condenser temperature of −110°C, chamber pressure of 0.1 mbar) using a bench top Freeze Dryer (SCANVAC Coolsafe model 110-4, Denmark). Increasing processing times between 2 and 48 hr were considered in the experiments (see Table 1), and for each experiment the moisture content (MC %) and water activity (a_w) of the samples were measured afterwards.

TABLE 1 Freeze-drying experimental results

t (hr)	MC% (w/w)	a_w
2	91.37 ± 1.04	0.9867 ± 0.0015
4	87.72 ± 1.39	0.9769 ± 0.0029
6	85.47 ± 2.43	0.9733 ± 0.0031
13	63.14 ± 3.06	0.7828 ± 0.0042
18	23.08 ± 3.35	0.2486 ± 0.0062
24	15.61 ± 1.56	0.2079 ± 0.0058
30	8.65 ± 0.91	0.1129 ± 0.0011
48	7.95 ± 0.78	0.1122 ± 0.0010

Note. Water activity and moisture content measured at different processing times for the fresh tomato samples

2.4 | Water activity analysis

Water activity (a_w) of fresh and dried samples was measured using an AquaLab dew point water activity meter (model 4TE, Decagon Devices, Inc., Pullman, WA) with controlled chamber temperature of 25°C. The measured water activity of the fresh samples was 0.9887 ± 0.0013. To prevent the proliferation of microorganisms, a_w should be reduced to values lower than 0.6 (de Bruijn et al., 2016).

2.5 | Microstructure

The structure of dried tomato samples was analyzed by X-ray microcomputed tomography (μCT). A Skyscan 1172 (Bruker μCT, Belgium) system was used to acquire three-dimensional images, which were subsequently reconstructed and processed (CT-analyzer 1.7.0.0) to obtain the porosity of the dried bulk structure and also the pore size distribution.

2.6 | Rehydration

Rehydration experiments were performed in triplicate by immersing a weighed amount of dried samples into distilled water at fixed temperature (i.e., 20, 40, and 50°C). At regular intervals, samples were removed from the medium, blotted with paper, and reweighed. Rehydration capacity (RC %) was measured for all the samples using the following equation (Meda & Ratti, 2005):

$$RC = 100 \times \frac{(w(t) - w_d)}{(w_0 - w_d)}, \quad (1)$$

where $w(t)$ is the weight of the sample at time t, w_d (g) is the weight of the dried sample, and w_0 (g) is the initial weight of the sample.

TABLE 2 Thin-layer drying models

Drying model	Expression		Application
Newton	$MR = e^{-k_1 t}$	Equation (2)	Red chili (Hossain & Bala, 2007); Strawberry (El-Beltagy, Gamea, & Essa, 2007)
Page	$MR = e^{-k_2 t^n}$	Equation (3)	Kiwifruit (Simal, 2005); Mango slices (Akoy, 2014)
Henderson and Pabis	$MR = a_1 e^{-k_3 t}$	Equation (4)	Apple slices (Meisami-asl, Rafiee, Keyhani, & Tabatabaeefar, 2010); Pumpkin (Hashim, Onwude, & Rahaman, 2014)
Logarithmic	$MR = a_2 e^{-k_4 t} + b_2$	Equation (5)	Basil leaves (Kadam, Goyal, & Gupta, 2011); Stone apple (Rayaguru & Routray, 2012)
Two-term	$MR = a_3 e^{-k_5 t} + b_3 e^{-k_6 t}$	Equation (6)	Fig (Babalis, Papanicolaou, Kyriakis, & Belessiotis, 2006); Plum (Jazini & Hatamipour, 2010)
Wang and Singh	$MR = 1 + k_7 t + k_8 t^2$	Equation (7)	Rough rice (Wang & Singh, 1978); Granny Smith apples (Blanco-Cano, Soria-Verdugo, Garcia-Gutierrez, & Ruiz-Rivas, 2016)

Note. Units for drying rate constants k_i are 1/hr, except for k_2 and k_8, which are $1/hr^n$ and $1/hr^2$, respectively.

2.7 | Drying kinetics modeling

The drying data obtained from the experiments were fitted to six well-known thin-layer drying models available in literature (Onwude et al., 2016): Newton (Henderson, 1974), Page (Page, 1949), Henderson and Pabis (Henderson, 1961), logarithmic (Karathanos, 1999), two-term (O. Ertekin & Yaldiz, 2001), and Wang and Singh (C. Wang & Singh, 1978). Table 2 lists all the models and their corresponding expressions.

The moisture ratio was calculated from the experimentally measured moisture content as follows:

$$MR = \frac{X(t) - X_{eq}}{X_0 - X_{eq}}, \tag{8}$$

where $X(t)$ is the moisture content in dry basis measured at different times (measured in hours for the freeze-drying experiments), X_0 is the initial moisture content (d.b), and X_{eq} is the equilibrium moisture content (d.b).

The equilibrium moisture content of the treated samples was calculated from the experimental water activity values using a Guggenheim-Anderson-DeBoer model (Van den Berg, 1984):

$$X_{eq} = \frac{X_m C K a_w}{(1 - K a_w)(1 - K a_w + C K a_w)}, \tag{9}$$

where the values of the monomolecular layer moisture content (d.b.) X_m, and the constants C and K were taken from literature (Belghith, Azzouz, & ElCafsi, 2016).

2.8 | Rehydration kinetics modeling

Rehydration kinetics of the freeze-dried tomatoes was described by four empirical models: Peleg, first-order kinetics, exponential, and Weibull. In the Peleg model (Peleg, 1988), the sample moisture content (d.b.) is defined as:

$$X(t) = X_0 + \frac{t}{k_9 + k_{10} t}, \tag{10}$$

where t is the time (in minutes, for the rehydration experiments), k_9 is the Peleg rate constant (a kinetic parameter), and k_{10} is the Peleg capacity constant, which is related to the equilibrium moisture content through the following equation:

$$X_{eq} = X_0 + \frac{1}{k_{10}}. \tag{11}$$

The exponential model is expressed as:

$$MR = \exp\left(-k_{11} t^{k_{12}}\right), \tag{12}$$

when $k_{12} = 1$, the exponential model becomes a first-order kinetic expression.

The Weibull distribution function is described by two parameters as reported in Equation (13):

$$\frac{X(t)}{X_{eq}} = 1 - \exp\left[-\left(\frac{t}{\alpha}\right)^{\beta}\right], \tag{13}$$

where α is the scale parameter (related to the reciprocal of the rate process) and β is the shape factor (Saguy, Marabi, & Wallach, 2005).

2.9 | Parameter estimation and model discrimination

Both for freeze-drying and rehydration the model parameters were evaluated by minimizing the error, e, between experimental (θ) and predicted (i.e., fitted) values ($\bar{\theta}$):

$$J = \sum_i^N e_i^2 = \sum_i^N (\theta_i - \bar{\theta}_i)^2, \tag{14}$$

where N represents the number of measurements in the experimental data set. In all cases, the least square method was employed and implemented using the function *lsqcurvefit* in Matlab with a tolerance of 10^{-10}.

Three different measures were employed to estimate the goodness-of-fit of each fitted model (Spiess & Neumeyer, 2010): adjusted R^2 (R^2_{adj}), corrected AIC (*AICC*), and the *BIC*. For all of them, the number of parameters p employed by each model was taken into account.

$$R^2_{adj} = 1 - \frac{N-1}{N-p}\left(1 - R^2\right), \tag{15}$$

$$AICC = AIC + \frac{2p(p+1)}{N-P-1}, \tag{16}$$

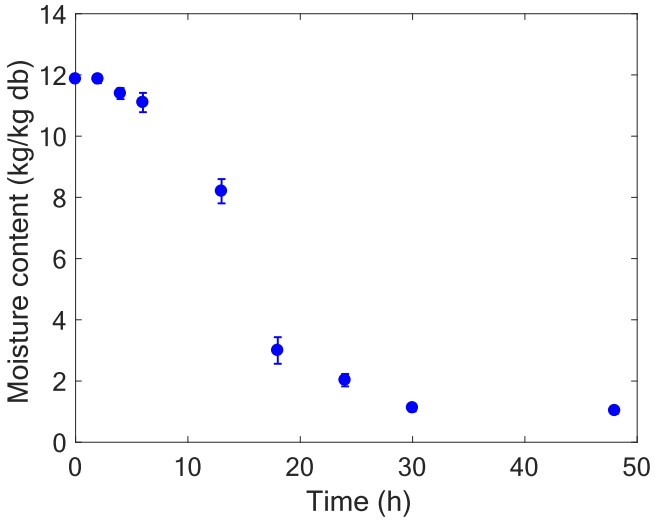

FIGURE 1 Drying curve corresponding to the freeze-dried tomato samples showing the variation of the moisture content (d.b.) over time. The freeze-drying experiments were performed in triplicate. The pressure chamber was held at 10 Pa and the condenser temperature was of −110°C

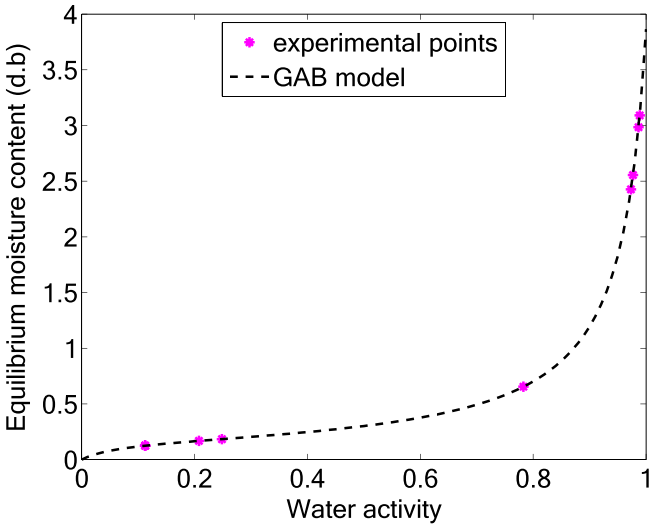

FIGURE 2 Equilibrium moisture content as a function of the water activity during the drying of the freeze-dried tomato samples. The graph also shows where the experimental a_w points lay on the GAB desorption curve (Belghith et al., 2016)

$$BIC = p\ln(N) - 2p\ln(L). \quad (17)$$

In Equations (15)–(17), R^2 is the regression coefficient of determination, *AIC* is the Akaike information criterion (Akaike, 1974; Moxon et al., 2017), and *L* is the maximum log-likelihood of the estimated model (Spiess & Neumeyer, 2010). The model with best performance will be defined by the higher R^2_{adj} and lower *AICC* and *BIC* values (J. Wang et al., 2013).

3 | RESULTS AND DISCUSSION

3.1 | Drying

Moisture content (% w.b.) and water activity were measured for 48 hr at different time intervals during the freeze-drying experiments. The values obtained alongside the corresponding standard deviation are shown in Table 1. The moisture content of the tomato samples remained close to the initial value during the first 6 hr of processing, as can be seen in Figure 1, where the drying curve (dry basis) is shown. Most of the water was removed—that is, ice was sublimated—during the next 24 hr of the process (corresponding to the steep slope in Figure 1), after which there were no significant changes and the moisture content remained almost constant at approx. 8% (w.b.). These three stages are typical of thin-layer drying profiles of fruits and vegetables (Onwude et al., 2016).

The experimental values measured for water activity of the system during drying (in Table 2) showed a similar behavior to that described for the moisture content, with a slow decay during the initial 6 hr of processing followed by a significant decrease over the next 24 hr. These experimental water activity values were employed to calculate the equilibrium moisture content X_{eq} of the tomato samples as described in Section 2.9. The theoretical desorption curve obtained is presented in Figure 2, which also shows experimental a_w values.

3.2 | Effect of processing conditions on the microstructure of the freeze-dried samples

To determine the influence of freeze-drying processes on the kinetics of water absorption during rehydration, it is key to ensure first that the resulting freeze-dried samples preserve its original microstructure and have not suffered matrix significant deformations (e.g., shrinkage, puffing, and collapse). Figure 3a shows a two-dimensional cross-section image of one of the freeze-dried tomato samples, where the cellular walls of the solid matrix appear as white/light gray and the voids left by the sublimation of the ice are the black regions. This cross-section image also shows that both phases—that is, the solid matrix and the voids—are structured in interconnected networks. The microstructure analysis provided values of porosity and mean pore size of the freeze-dried samples equal to 83% and ≈100–125 μm (Figure 3b), respectively. This pore size suggests no signs of damage in the tomato microstructure: fresh tomato cell mean size is ~100 μm (Corrêa, Justus, De Oliveira, & Alves, 2015), a value in the same range than the analyzed freeze-dried samples.

In order to avoid the collapse of the freeze-dried structure (i.e., softening, shrinkage, loss of porosity, and structure integrity), product temperature must be above the glass transition temperature during freezing and below the collapse temperature, T_{col}, during the sublimation stage (Ratti, 2012). According to literature, T'_g = −59°C for freeze-dried tomatoes (Telis & Sobral, 2002). Thus, the first condition has been largely fulfilled by choosing a temperature T_{fr} = −20°C to freeze the samples, as detailed in Section 2.3.

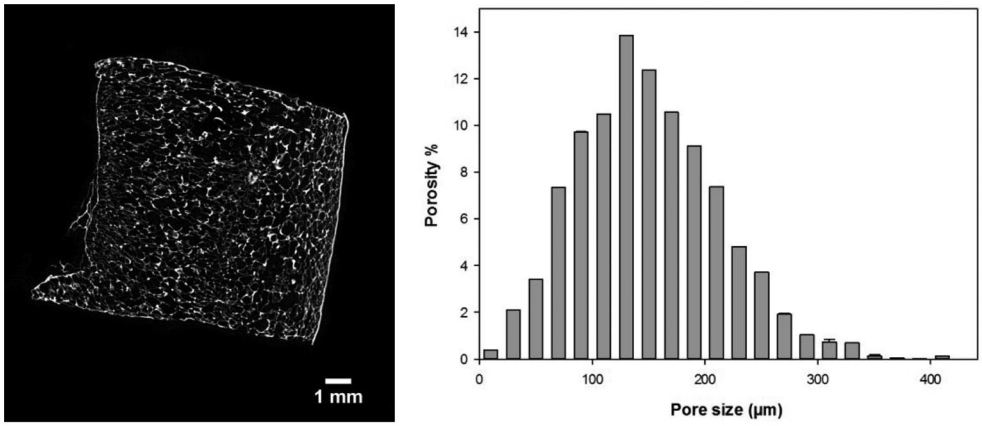

(a) (b)

FIGURE 3 (a) Two-dimensional cross section of a freeze-dried tomato sample obtained from μCT analysis. The cellular walls in the image are the white/light gray regions, while the pores are the black ones. (b) Corresponding pore size distribution, with a mean pore size of ~125 μm. μCT, microcomputed tomography

During the sublimation stage, product collapse can be avoided by adjusting the chamber pressure P_c (Ratti, 2012) so that $T_{prod} < T_{col} = -41°C$ (Ratti, 2001). At this stage, the product temperature T_{prod} can be calculated from the combination of the Clausius–Clapeyron relationship (Ibarz & Barbosa-Cánovas, 2002):

$$\ln P_{sub} = 30.9526 - \frac{6,153.1}{T_{sub}}, \quad (18)$$

where P_{sub} (Pa) is the sublimation pressure, T_{sub} (K) is the sublimation temperature, and the following expression derived from energy and mass balances across the sublimation front (Ibarz & Barbosa-Cánovas, 2002):

$$P_{sub} = P_c + \frac{\rho_{fr}\left(x_w^{ini} - x_w^{fin}\right)a^2}{2K_p\left(1 + x_w^{ini}\right)t_{sub}}, \quad (19)$$

where x_w^{ini} and x_w^{fin} are the initial and final moisture contents (dry basis), respectively, ρ_{fr} (kg/m^3) is the density of the frozen layer, a^2 is the thickness of the half-slab, t_{sub} (s) is the sublimation time, and K_p (kg/msPa) is the permeability of the dry material. Equation (19) was employed to obtain T_{col} and T'_g bounds for a range of operational conditions (e.g., P_c and t_{sub}) and sample thickness ($2a$) using $K_p = 1.58 \times 10^{-8}$ kg/msPa for tomatoes (Ibarz & Barbosa-Cánovas, 2002) and considering $\rho_{fr} \simeq \rho_{ice}$. Results shown in Figure 4 indicate that, for a given P_c value and increasing sample thickness, longer sublimation times are needed to achieve the same final moisture content. Also, for a fixed sample thickness, sublimation times can be reduced by working at lower chamber pressures. For the freeze-drying process detailed in Section 2.3, a value of $T_{sub} = -57°C < T_{col}$ was obtained, which together with the results of the microtomography analysis, can be used to demonstrate both product structure integrity and suitability of the freeze-drying cycle implemented in this work. Such critical point in the analysis of rehydration kinetics in freeze-dried tomato matrices has not been recognized in previous publications (Chawla et al., 2008; Gaware et al., 2010; Krokida & Philippopoulos, 2005).

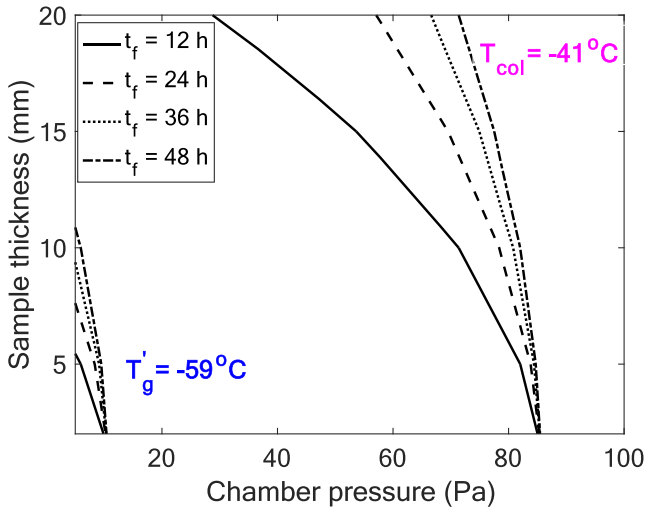

FIGURE 4 Operational bounds—lower (T'_g) and higher (T_{col})—given by Equation (19) for the sublimation stage/primary drying of tomatoes as function of time t_{sub}, pressure chamber P_c, and sample thickness ($2a$). It has been assumed that $\rho_{fr} \simeq \rho_{ice}$ and $K_p = 1.58 \times 10^{-8}$kg/sPam. Initial and final moisture contents were taken from Table 1 and converted into dry basis values

3.3 | Parameter estimation of drying constants and thin-later models discrimination

Table 3 lists the estimated parameters for the six thin-layer models for drying kinetics described in Section 2.8, alongside with the root mean square error (*RMSE*) of each fitting. In this table, the results corresponding to the goodness-of-fit of each model are also presented. According to the calculated R^2_{adj} (0.98), *AICC* (−21.283), and *BIC* (−22.889) values, the Page model provides the most accurate description of the drying kinetics, representing correctly the three observed stages of the drying process. This is in agreement with Chawla et al. (2008) and also with Gaware et al. (2010), who also described freeze-drying kinetics using the Page's model (results cannot be compared as drying configurations and operation conditions are different to those employed in this work). The goodness of the fitted Page model is illustrated in Figure 5, where experimental values are plotted against predicted

TABLE 3 Regression and goodness-of-fit results: Drying kinetics

Model	Parameters	*RMSE*	R^2_{adj}	BIC	AICC
Newton	k_1 = 0.054	0.129	0.903	−10.129	−9.755
Page	k_2 = 0.016; n = 2.253	0.056	0.979	−22.889	−21.283
Henderson	a_1 = 1.126; k_3 = 0.062	0.111	0.918	−10.733	−9.128
Logarithmic	a_2 = 1.239; k_4 = 0.050; b_2 = −0.129	0.106	0.913	−9.363	−5.155
Two-term	a_3 = 0.167; k_5 = 0.062; b_3 = 0.959; k_6 = 0.062	0.111	0.886	−6.339	2.872
Wang and Singh	k_7 = −0.044; k_8 = 0.0005	0.106	0.926	−11.554	−9.948

Abbreviations: AICC, corrected Akaike information criterion; BIC, Bayesian information criterion; RMSE, root mean square error.

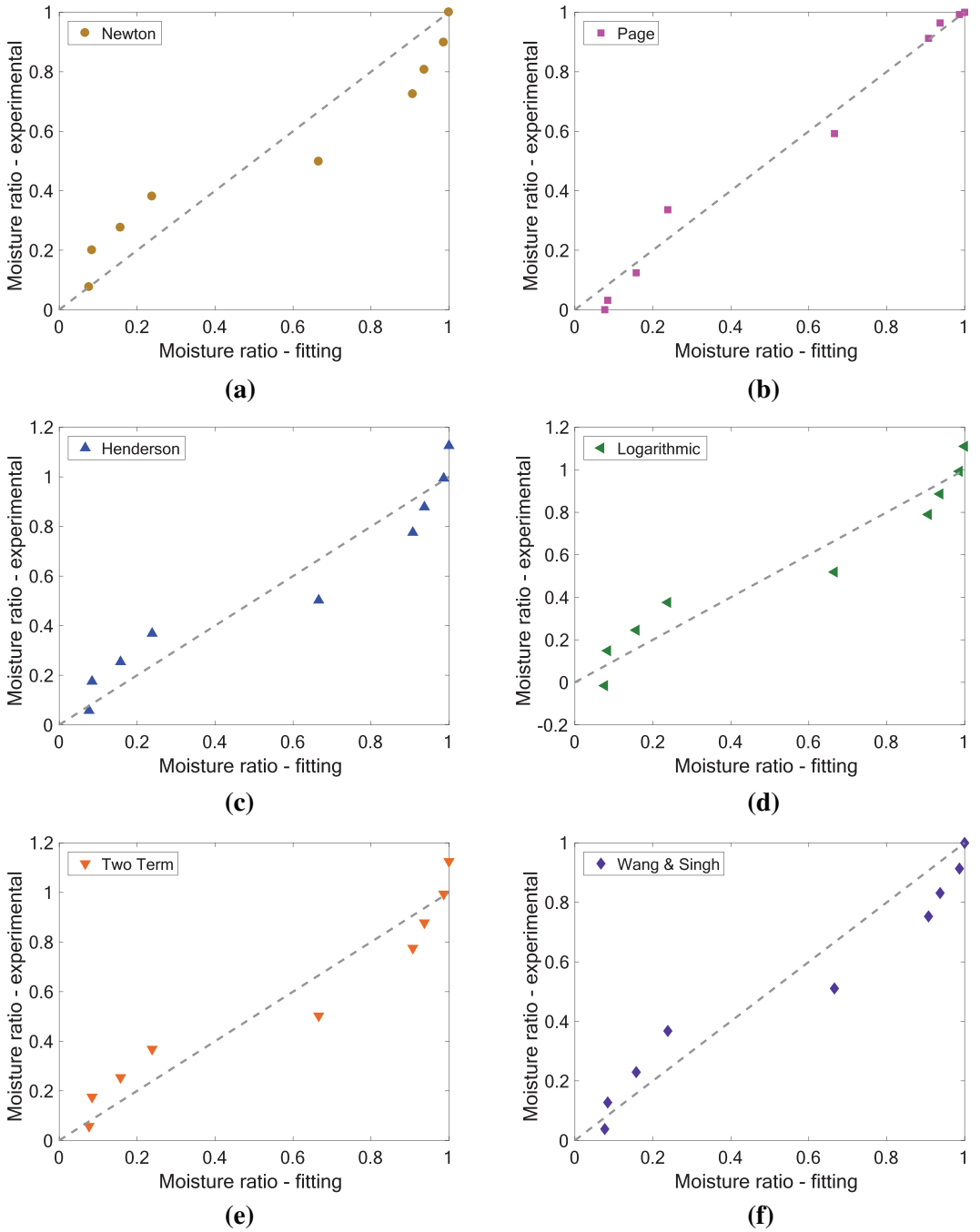

FIGURE 5 (a) Newton model [Equation (2)], (b) Page model [Equation (3)], (c) Henderson and Pabis model [Equation (4)], (d) logarithmic model [Equation (5)], (e) two-term model [Equation (6)], and (f) Wang and Singh model [Equation (7)]. Experimental data are also shown (points are averages of the presented in Figure 1)

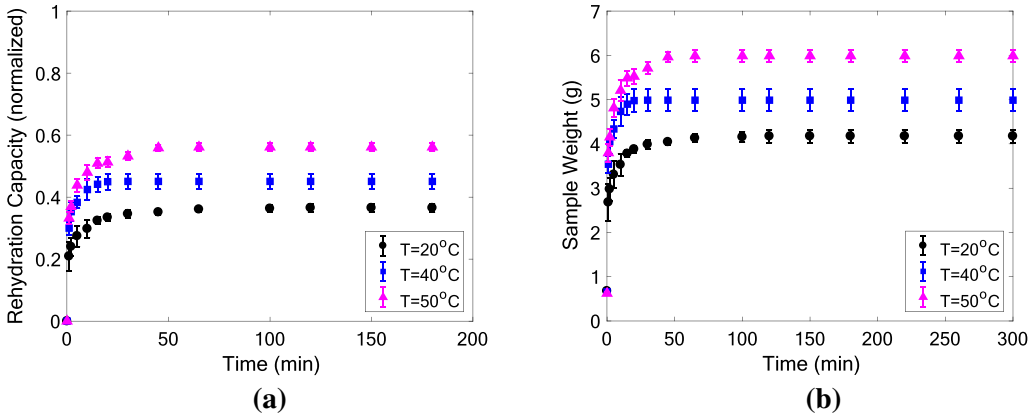

FIGURE 6 Rehydration curves corresponding to medium temperatures of 20°C (crosses), 40°C (circles), and 50°C (triangles). Higher temperature resulted in higher rehydration capacities

TABLE 4 Regression and goodness-of-fit results: Rehydration kinetics

Model	Temperature	Parameters	RMSE	R^2_{adj}	BIC	AICC
Peleg						
	20°C	$k_9 = 0.231; k_{10} = 0.179$	*0.232*	*0.976*	*2.077*	*1.268*
	40°C	$k_9 = 0.090; k_{10} = 0.141$	*0.117*	*0.996*	*−21.302*	*−22.111*
	50°C	$k_9 = 0.095; k_{10} = 0.110$	*0.290*	*0.985*	*9.708*	*8.898*
Exponential						
	20°C	$k_{11} = 0.704; k_{12} = 0.380$	*0.064*	*0.998*	*−41.929*	*−42.738*
	40°C	$k_{11} = 1.003; k_{12} = 0.442$	*0.068*	*0.999*	*−39.622*	*−40.431*
	50°C	$k_{11} = 0.885; k_{12} = 0.367$	*0.093*	*0.998*	*−28.892*	*−29.701*
First-order						
	20°C	$k_{13} = 0.442$	*0.516*	*0.880*	*27.538*	*26.971*
	40°C	$k_{13} = 0.824$	*0.324*	*0.967*	*11.681*	*11.114*
	50°C	$k_{13} = 0.645$	*0.660*	*0.920*	*35.931*	*35.364*
Weibull						
	20°C	$\alpha = 2.417; \beta = 0.376$	*0.068*	*0.998*	*−39.782*	*−40.591*
	40°C	$\alpha = 0.968; \beta = 0.439$	*0.072*	*0.999*	*−37.914*	*−38.723*
	50°C	$\alpha = 1.365; \beta = 0.364$	*0.096*	*0.998*	*−27.833*	*−28.642*

Abbreviations: AICC, corrected Akaike information criterion; BIC, Bayesian information criterion; RMSE, root mean square error.

moisture ratios for each drying model. Kinetics models based on Fick's second law (i.e., Henderson, logarithmic, and two-term) systematically overestimated the initial water content. Wang and Singh model—an empirical one—could predict both initial and final moisture contents, although failed in describing the characteristic drying stages experimentally observed.

The number of parameters involved in the thin-layer models studied in this work ranges from $p = 1$ (Newton) to $p = 4$ (two term). When comparing models with similar accuracies, the *AICC* criterion constitutes the best measure to discriminate models. For the drying kinetics of the freeze-dried tomatoes, the Henderson ($p = 2$) and the logarithmic ($p = 3$) models in Table 3 present similar R^2_{adj} values. However, the most negative *AICC* value corresponds to the model with fewer parameters [i.e., the Henderson in Equation (4)]. Accordingly, the two-term model [Equation (6)] is strongly affected by its complexity (i.e., number of parameters, with $p = 4$), presenting the highest *AICC* (2.872).

3.4 | Rehydration

Rehydration curves related to experiments carried out at 20, 40, and 50°C are reported in Figure 6. The observed trends suggest a diffusion-controlled process (Maldonado, Arnau, & Bertuzzi, 2010; Peleg, 1988; Turhan, Sayar, & Gunasekaran, 2002). Independently from the temperature of the medium investigated, all dried samples showed fast rehydration in the first minutes, followed by slower water absorption, which achieved the equilibrium after ~50 min. Rehydration rate was found to be about four time faster than that observed for hot air-dried tomatoes (Goula & Adamopoulos, 2009; Krokida & Marinos-Kouris, 2003) and six times faster than infrared dried tomatoes (Doymaz, 2014).

Increasing the temperature of the rehydration medium resulted in higher rehydration capacities and, therefore, higher final equilibrium moisture contents: *RC* equal to 52% was observed at 50°C, whereas

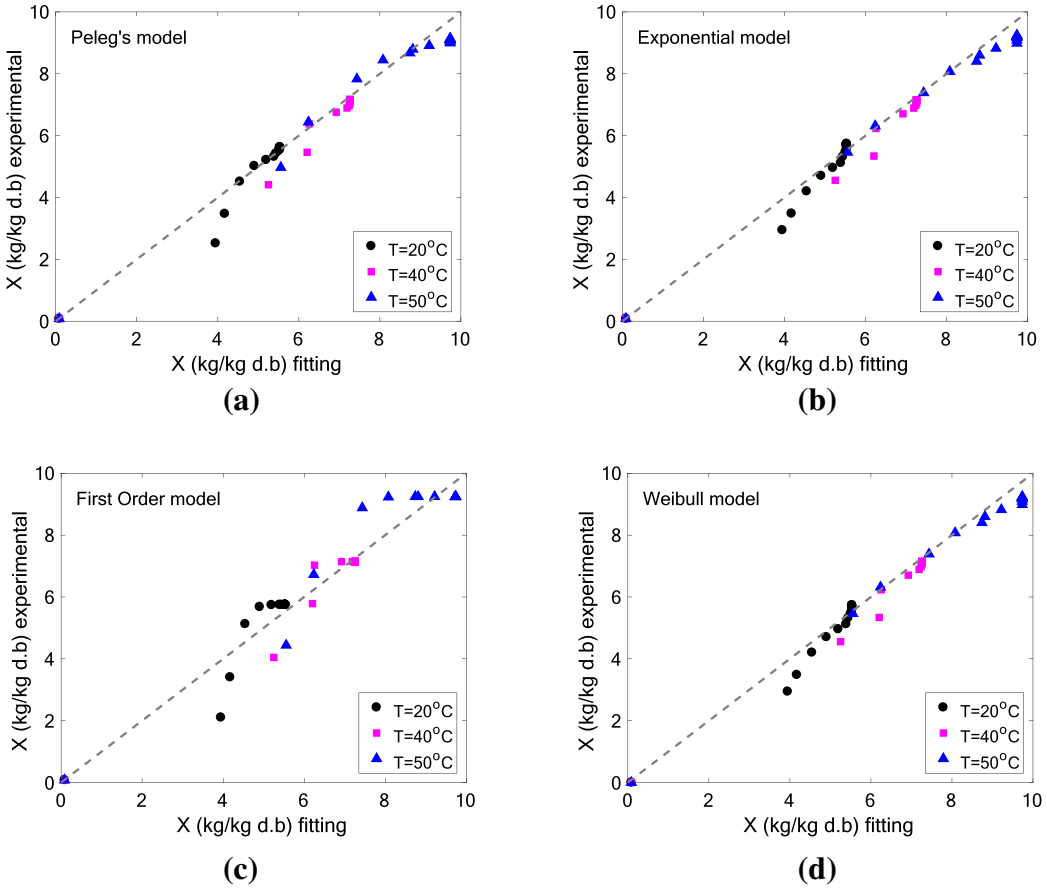

FIGURE 7 Correlation between predicted and experimental moisture contents (d.b.) for: (a) Peleg's model [Equation (10)], (b) exponential model [Equation (12)], (c) first-order model [Equation (12) and k_{12} = 1], and (d) Weibull model [Equation (13)]

only 37% was achieved at 20°C. Nevertheless, rehydrated samples did not reach the initial moisture content (fresh tomatoes), suggesting the irreversibility of the drying process (Krokida & Philippopoulos, 2005). Krokida and Marinos-Kouris (2003) also observed a positive effect of temperature on rehydration of air-dried tomatoes: with increasing the temperature, higher degree of swelling occurs, and diffusion thorough cell walls of noninterconnected pores is promoted. Conversely, Gaware et al. (2010) reported very similar rehydration behaviors at T = 25°C and T = 100°C for freeze-dried tomatoes. Given the significant difference between both temperatures, such results can only be explained by a damaged (collapsed, nonporous) tomato freeze-dried matrix that has prevented water absorption (Krokida & Philippopoulos, 2005).

Ultimately, in this work, freeze-dried tomatoes showed higher RC (up to 58% at 50°C) compared to hot-air dried tomatoes (around 30%, at temperatures ranging between 25 and 80°C; according to Goula and Adamopoulos [2009]).

3.5 | Rehydration kinetics: Parameter estimation and model discrimination

Table 4 shows the rehydration parameters corresponding to the empirical models considered in this work: Peleg, exponential, first-order kinetics, and Weibull. For freeze-dried tomatoes, he estimated values of the Weibull's shape factor β (~0.4) do not match expected values for either Fickian (~0.8) or non-Fickian diffusion mechanisms (~0.6), which suggests that capillary flow may occur, as already observed by Marabi, Livings, Jacobson, and Saguy (2003) for freeze-dried carrots. This is supported by the fact that the times corresponding to the fast initial water absorption observed during the rehydration tests (5–10 s; see Figure 6) are in agreement with the capillary suction time-scale (≈ 6 s) predicted by Van der Sman et al. (2014) during the rehydration of freeze-dried foods.

In Table 4, the corresponding values of *RMSE*, R^2_{adj}, *AICC*, and *BIC* are also reported, whereas in Figure 7, the experimental data are plotted against the predicted moisture contents. The first-order model (Figure 7c) led to the lowest R^2_{adj}; this suggests that a single kinetic constant is not sufficient to describe accurately the initial fast absorption rate and the subsequent relaxation of the system. The exponential model (p = 2) shows the highest R^2_{adj} and the lowest *AICC* and *BIC* values and, therefore, represents the most accurate to describe the rehydration kinetics of freeze-dried tomatoes, followed by the Weibull model. In Figure 7b,d, the accuracy of these two models can be appreciated: most of the points lie on the correlation line.

3.6 | Effect of temperature on rehydration kinetics

The influence of temperature on the equilibrium moisture content of the rehydrated samples is reflected on the values of the Peleg's

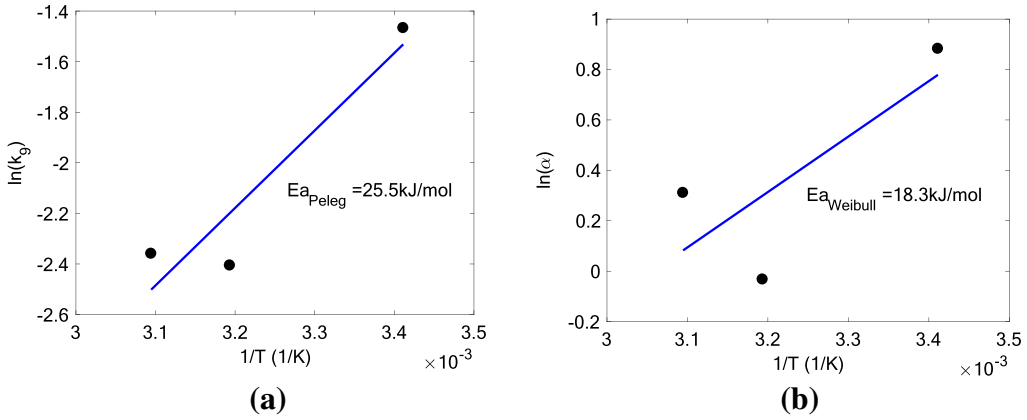

FIGURE 8 Effect of temperature on rehydration rate according to (a) Peleg's model and (b) Weibull model alongside calculated activation energy values for the system

capacity constant k_{10}. This constant is inversely proportional to the sample rehydration capacity (Khazaei & Mohammadi, 2009), leading to decreasing values for increasing temperatures, as those reported in Table 4 for the freeze-dried tomatoes are attributed to higher equilibrium moisture contents in the rehydrated samples (see Figure 4).

Peleg's rate constant k_9 and Weibull's scale parameter α are both related to the water absorption rate of the system: the terms $1/k_9$ and $1/\alpha$ are higher in systems with faster initial rates. For the system under investigation, both Peleg and Weibull rate parameters show the same trend, with the fastest initial rehydration rate corresponding to medium temperatures of 40°C and the slowest rate corresponding to rehydration at 20°C.

In order to estimate the overall effect of temperature on the rehydration kinetics, the natural logarithmic of the Peleg and Weibull rate constants were plotted as a function of the inverse of the temperature $1/T$, as shown in Figure 8a,b, respectively. Very similar system behavior was observed at 40 and 50°C, with corresponding points very close for both Peleg and Weibull model predictions. The activation energy E_a (KJ/mol) of rehydration was calculated as the slope of the best linear fitting to the data. Analogous values were again attained from both Peleg and Weibull constants: E_{a_Peleg} = 25.5 kJ/mol and $E_{a\_Weibull}$ = 18.3 kJ/mol. No other works studying rehydration kinetics of freeze-dried tomatoes (i.e., Gaware et al., 2010; Krokida & Philippopoulos, 2005) have reported energy activation values. However, the values presented in this work are in agreement with reported data for air-dried and rehydrated tomatoes (Doymaz & Özdemir, 2014) and other vegetables (spinach in Dadali, Demirhan, and Özbek [2008]; green peas in Doymaz and Kocayigit [2011; morel in García-Pascual, Sanjuán, Melis, and Mulet [2006]).

4 | CONCLUSIONS

In this work, drying and rehydration kinetics of freeze-dried tomatoes were experimentally investigated and modeled. The Page model revealed to be the most accurate in describing of the drying kinetics, whereas both exponential and Weibull models reliably predicted the initial fast water absorption rates and subsequent relaxation that were observed in the rehydration of the freeze-dried tomatoes.

In addition, it was observed that the temperature of the medium had a strong influence on the rehydration process—the higher the temperature, the higher the rehydration capacities and equilibrium moisture contents; this is indicated by both the experimental rehydration curves and the estimated Peleg capacity constant. The estimated Peleg's and Weibull's rate constants were used to calculate the activation energy for rehydration, and values in agreement with the existing literature were obtained. In addition, the estimated values of Weibull's shape parameter suggested the occurrence of a capillary flow contribution to water absorption at the beginning of the rehydration process, which can also explain the initial fast absorption rates observed.

Overall, the comprehensive model-based study presented in this work demonstrated that a highly interconnected porous microstructure, such that resulting from the designed-for-quality freeze-drying approach used here, can promote fast rehydration rate in dried tomatoes. These results set the basis for a supply scenario based on distributive manufacturing principles, where freeze-dried foods could be first distributed and then rehydrated closer to the consumption point.

ACKNOWLEDGMENTS

Authors would like to thank the financial support received from EPSRC (grant numbers EP/K011820/1 and EP/K030957/1).

ORCID

Valentina Prosapio https://orcid.org/0000-0003-1311-2055

REFERENCES

Akaike, H. (1974). A new look at the statistical model identification. *IEEE Transactions on Automatic Control*, *19*(6), 716–723.

Akoy, E. (2014). Experimental characterization and modeling of thin-layer drying of mango slices. *International Food Research Journal*, *21*(5), 1911–1917.

Alfat, S., & Purqon, A. (2017). Heat and mass transfer model in freeze-dried medium. *Journal of Physics: Conference Series*, *877*, 1–7.

Almena, A., Fryer, P. J., Bakalis, S., & Lopez-Quiroga, E. (2019). Centralized and distributed food manufacture: A modeling platform for technological, environmental and economic assessment at different production scales. *Sustainable Production and Consumption*, *19*, 181–193.

Andrieu, J., & Vessot, S. (2018). A review on experimental determination and optimization of physical quality factors during pharmaceuticals freeze-drying cycles. *Drying Technology*, *36*(2), 129–145.

Babalis, S. J., Papanicolaou, E., Kyriakis, N., & Belessiotis, V. G. (2006). Evaluation of thin-layer drying models for describing drying kinetics of figs (Ficus carica). *Journal of Food Engineering*, *75*(2), 205–214.

Baldea, M., Edgar, T. F., Stanley, B. L., & Kiss, A. A. (2017). Modular manufacturing processes: Status, challenges and opportunities. *AICHE Journal*, *63*(10), 4262–4272.

Belghith, A., Azzouz, S., & ElCafsi, A. (2016). Desorption isotherms and mathematical modeling of thin layer drying kinetics of tomato. *Heat and Mass Transfer/Waerme-Und Stoffuebertragung*, *52*(3), 407–419. https://doi.org/10.1007/s00231-015-1560-0

Blanco-Cano, L., Soria-Verdugo, A., Garcia-Gutierrez, L. M., & Ruiz-Rivas, U. (2016). Modeling the thin-layer drying process of Granny Smith apples: Application in an indirect solar dryer. *Applied Thermal Engineering*, *108*, 1086–1094.

Bosca, S., Barresi, A., & Fissore, D. (2016). On the use of model-based tools to optimize in-line a pharmaceuticals freeze-drying process. *Drying Technology*, *34*(15), 1831–1842.

Bourdoux, S., Li, D., Rajkovic, A., Devlieghere, F., & Uyttendaele, M. (2016). Performance of drying technologies to ensure microbial safety of dried fruits and vegetables. *Comprehensive Reviews in Food Science and Food Safety*, *15*(6), 1056–1066.

Chawla, C., Kaur, D., Oberoi, D., & Sogi, D. (2008). Drying characteristics, sorption isotherms, and lycopene retention of tomato pulp. *Drying Technology*, *26*(10), 1257–1264.

Colucci, D., Fissore, D., Mulet, A., & Cárcel, J. A. (2017). On the investigation into the kinetics of the ultrasound-assisted atmospheric freeze drying of eggplant. *Drying Technology*, *35*(15), 1818–1831.

Corrêa, J. L. G., Justus, A., De Oliveira, L. F., & Alves, G. E. (2015). Osmotic dehydration of tomato assisted by ultrasound: Evaluation of the liquid media on mass transfer and product quality. *International Journal of Food Engineering*, *11*(4), 505–516. https://doi.org/10.1515/ijfe-2015-0083

Dadali, G., Demirhan, E., & Özbek, B. (2008). Effect of drying conditions on rehydration kinetics of microwave dried spinach. *Food and Bioproducts Processing*, *86*(4), 235–241.

de Bruijn, J., Rivas, F., Rodriguez, Y., Loyola, C., Flores, A., Melin, P., & Borquez, R. (2016). Effect of vacuum microwave drying on the quality and storage stability of strawberries. *Journal of Food Processing and Preservation*, *40*, 1104–1115. https://doi.org/10.1111/jfpp.12691

Doymaz, İ. (2014). Mathematical modeling of drying of tomato slices using infrared radiation. *Journal of Food Processing and Preservation*, *38*(1), 389–396.

Doymaz, İ., & Kocayigit, F. (2011). Drying and rehydration behaviors of convection drying of green peas. *Drying Technology*, *29*(11), 1273–1282.

Doymaz, İ., & Özdemir, Ö. (2014). Effect of air temperature, slice thickness and pretreatment on drying and rehydration of tomato. *International Journal of Food Science & Technology*, *49*(2), 558–564.

El-Beltagy, A., Gamea, G., & Essa, A. A. (2007). Solar drying characteristics of strawberry. *Journal of food engineering*, *78*(2), 456–464.

Ertekin, C., & Firat, M. Z. (2017). A comprehensive review of thin-layer drying models used in agricultural products. *Critical Reviews in Food Science and Nutrition*, *57*(4), 701–717.

Ertekin, O., & Yaldiz, C. (2001). Thin layer solar drying of some different vegetables. *Drying Technology*, *19*, 583–596.

FAO. (2014). FAOSTAT. Retrieved from http://faostat.fao.org/beta/en/#data/QC.

García-Pascual, P., Sanjuán, N., Melis, R., & Mulet, A. (2006). Morchella esculenta (morel) rehydration process modelling. *Journal of Food Engineering*, *72*(4), 346–353.

Gaware, T., Sutar, N., & Thorat, B. (2010). Drying of tomato using different methods: Comparison of dehydration and rehydration kinetics. *Drying Technology*, *28*(5), 651–658.

Goula, A. M., & Adamopoulos, K. G. (2009). Modeling the rehydration process of dried tomato. *Drying Technology*, *27*(10), 1078–1088.

Hashim, N., Onwude, D., & Rahaman, E. (2014). A preliminary study: kinetic model of drying process of pumpkins (Cucurbita moschata) in a convectivehot air dryer. *Agric Agric Sci Procedia*, *2*(2), 345–352.

Henderson, S. (1961). Grain drying theory temperature effect of drying coefficient. *Journal of Agricultural Engineering Research*, *6*, 169–174.

Henderson, S. (1974). Progress in developing the thin layer drying equation. *Transactions of ASAE*, *17*(6), 1167–1168.

Hossain, M., & Bala, B. (2007). Drying of hot chilli using solar tunnel drier. *Solar Energy*, *81*(1), 85–92.

Ibarz, A., & Barbosa-Cánovas, G. V. (2002). *Unit operations in food engineering*. Bosa Roca, United States: CRC Press.

Jazini, M., & Hatamipour, M. (2010). A new physical pretreatment of plum for drying. *Food and Bioproducts Processing*, *88*(2–3), 133–137.

Joardder, M. U., Kumar, C., & Karim, M. (2017). Food structure: Its formation and relationships with other properties. *Critical Reviews in Food Science and Nutrition*, *57*(6), 1190–1205.

Kadam, D., Goyal, R., & Gupta, M. (2011). Mathematical modeling of convective thin layer drying of basil leaves. *Journal of Medicinal Plants Research*, *5*(19), 4721–4730.

Karam, M. C., Petit, J., Zimmer, D., Baudelaire Djantou, E., & Scher, J. (2016). Effects of drying and grinding in production of fruit and vegetable powders: A review. *Journal of Food Engineering*, *188*, 32–49. https://doi.org/10.1016/j.jfoodeng.2016.05.001

Karathanos, V. T. (1999). Determination of water content of dried fruits by drying kinetics. *Journal of Food Engineering*, *39*(4), 337–344.

Karathanos, V. T., Anglea, S., & Karel, M. (1996). Structural collapse of plant materials during freeze-drying. *Journal of Thermal Analysis and Calorimetry*, *47*(5), 1451–1461.

Khalloufi, S., & Ratti, C. (2003). Quality deterioration of freeze-dried foods as explained by their glass transition temperature and internal structure. *Journal of Food Science*, *68*(3), 892–903.

Khazaei, J., & Mohammadi, N. (2009). Effect of temperature on hydration kinetics of sesame seeds (*Sesamum indicum* L.). *Journal of Food Engineering*, *91*(4), 542–552.

Krokida, M. K., & Marinos-Kouris, D. (2003). Rehydration kinetics of dehydrated products. *Journal of Food Engineering*, *57*(1), 1-7. doi: https://doi.org/10.1016/S0260-8774(02)00214-5

Krokida, M. K., & Philippopoulos, C. (2005). Rehydration of dehydrated foods. *Drying Technology*, *23*(4), 799–830.

Ladha-Sabur, A., Bakalis, S., Fryer, P. J., & Lopez-Quiroga, E. (2019). Mapping energy consumption in food manufacturing. *Trends in Food Science and Technology*, *86*, 270–280.

Lewicki, P. P., H. V. Le, & W. Pomarańska-Łazuka. (2002). Effect of pretreatment on convective drying of tomatoes. *Journal of Food Engineering*, *54*(2), 141–146. doi:https://doi.org/10.1016/S0260-8774(01)00199-6

Lewicki, P. P., & Wiczkowska, J. (2006). Rehydration of apple dried by different methods. *International Journal of Food Properties*, *9*(2), 217–226.

Link, J. V., Tribuzi, G., & Laurindo, J. B. (2017). Improving quality of dried fruits: A comparison between conductive multi-flash and traditional drying methods. *LWT- Food Science and Technology*, *84*, 717–725.

Lopez-Quiroga, E., L. T. Antelo, & A. A. Alonso. (2012). Time-scale modeling and optimal control of freeze–drying. *Journal of Food Engineering*, *111*(4), 655–666.

Lopez-Quiroga, E., Wang, R., Gouseti, O., Fryer, P., & Bakalis, S. (2016). Crystallisation in concentrated systems: A modelling approach. *Food and Bioproducts Processing*, *100*, 525–534.

Maldonado, S., Arnau, E., & Bertuzzi, M. (2010). Effect of temperature and pretreatment on water diffusion during rehydration of dehydrated mangoes. *Journal of Food Engineering*, *96*(3), 333–341.

Marabi, A., Livings, S., Jacobson, M., & Saguy, I. (2003). Normalized Weibull distribution for modeling rehydration of food particulates. *European Food Research and Technology*, *217*(4), 311–318.

Marabi, A., & Saguy, I. S. (2004). Effect of porosity on rehydration of dry food particulates. *Journal of the Science of Food and Agriculture*, *84*(10), 1105–1110.

Marques, L. G., Prado, M. M., & Freire, J. T. (2009). Rehydration characteristics of freeze-dried tropical fruits. *LWT-Food Science and Technology*, *42*(7), 1232–1237.

Meda, L., & Ratti, C. (2005). Rehydration of freeze-dried strawberries at varying temperatures. *Journal of Food Process Engineering*, *28*(3), 233–246.

Meisami-asl, E., Rafiee, S., Keyhani, A., & Tabatabaeefar, A. (2010). Drying of apple slices (var. Golab) and effect on moisture diffusivity and activation energy. *Plant Omics*, *3*(3), 97.

Moxon, T. E., Nimmegeers, P., Telen, D., Fryer, P. J., Van Impe, J., & Bakalis, S. (2017). Effect of chyme viscosity and nutrient feedback mechanism on gastric emptying. *Chemical Engineering Science*, *171*, 318–330.

Omolola, A. O., Jideani, A. I., & Kapila, P. F. (2017). Quality properties of fruits as affected by drying operation. *Critical Reviews in Food Science and Nutrition*, *57*(1), 95–108.

Onwude, D. I., Hashim, N., Janius, R. B., Nawi, N. M., & Abdan, K. (2016). Modeling the thin-layer drying of fruits and vegetables: A review. *Comprehensive Reviews in Food Science and Food Safety*, *15*(3), 599–618.

Page, G. E. (1949). *Factors influencing the maximum rates of air drying shelled corn in thin layers*. M.S thesis, Purdue University.

Peleg, M. (1988). An empirical model for the description of moisture sorption curves. *Journal of Food Science*, *53*(4), 1216–1217.

Prosapio, V., & Norton, I. (2017). Influence of osmotic dehydration pretreatment on oven drying and freeze drying performance. *LWT-Food Science and Technology*, *80*, 401–408. https://doi.org/10.1016/j.lwt.2017.03.012

Prosapio, V., & Norton, I. (2018). Simultaneous application of ultrasounds and firming agents to improve the quality properties of osmotic + freeze-dried foods. *LWT*, *96*, 402–410. https://doi.org/10.1016/j.lwt.2018.05.068

Prosapio, V., Norton, I., & De Marco, I. (2017). Optimization of freeze-drying using a life cycle assessment approach: Strawberries' case study. *Journal of Cleaner Production*, *168*, 1171–1179. https://doi.org/10.1016/j.jclepro.2017.09.125

Qiao, F., Fang, C., Huang, L., & Zhang, S. (2013). The effect of different heating patterns on vacuum freeze-drying of litchi pulp. *Journal of Food Process Engineering*, *36*(4), 407–411.

Ratti, C. (2001). Hot air and freeze-drying of high-value foods: A review. *Journal of Food Engineering*, *49*, 311–319. https://doi.org/10.1016/S0260-8774(00)00228-4

Ratti, C. (2012). Freeze-drying process design. *Handbook of Food Process Design*, chapter 22, 621–647.

Rayaguru, K., & Routray, W. (2012). Mathematical modeling of thin layer drying kinetics of stone apple slices.

Roos, Y. H., Fryer, P. J., Knorr, D., Schuchmann, H. P., Schroën, K., Schutyser, M. A. I., … Windhab, E. J. (2016). Food engineering at multiple scales: Case studies, challenges and the future—A European perspective. *Food Engineering Reviews*, *8*(2), 91–115. https://doi.org/10.1007/s12393-015-9125-z

Sagar, V. R., & Suresh Kumar, P. (2010). Recent advances in drying and dehydration of fruits and vegetables: A review. *Journal of Food Science and Technology*, *47*(1), 15–26. https://doi.org/10.1007/s13197-010-0010-8

Saguy, I. S., Marabi, A., & Wallach, R. (2005). New approach to model rehydration of dry food particulates utilizing principles of liquid transport in porous media. *Trends in Food Science & Technology*, *16*(11), 495–506.

Sampaio, R. M., Neto, J. P. M., Perez, V. H., Marcos, S. K., Boizan, M. A., & Silva, L. R. (2017). Mathematical Modeling of drying kinetics of persimmon fruits (*Diospyros kaki* cv. Fuyu). *Journal of Food Processing and Preservation*, *41*(1), 1–7.

Spiess, A.-N., & Neumeyer, N. (2010). An evaluation of R 2 as an inadequate measure for nonlinear models in pharmacological and biochemical research: A Monte Carlo approach. *BMC Pharmacology*, *10*(1), 6.

Tarafdar, A., Shahi, N. C., Singh, A., & Sirohi, R. (2018). Artificial neural network Modeling of water activity: A low energy approach to freeze drying. *Food and Bioprocess Technology*, *11*(1), 164–171.

Telis, V., & Sobral, P. (2002). Glass transitions for freeze-dried and air-dried tomato. *Food Research International*, *35*(5), 435–443.

Turhan, M., Sayar, S., & Gunasekaran, S. (2002). Application of Peleg model to study water absorption in chickpea during soaking. *Journal of Food Engineering*, *53*(2), 153–159.

Van den Berg, C. (1984). Description of water activity of foods for engineering purposes by means of the GAB model of sorption. *Engineering Science in the Food Industry*, *24*, 311–321.

Van der Sman, R., Vergeldt, F., Van As, H., Van Dalen, G., Voda, A., & Van Duynhoven, J. (2014). Multiphysics pore-scale model for the rehydration of porous foods. *Innovative Food Science & Emerging Technologies*, *24*, 69–79.

Vega-Gálvez, A., Zura-Bravo, L., Lemus-Mondaca, R., Martinez-Monzó, J., Quispe-Fuentes, I., Puente, L., & Di Scala, K. (2015). Influence of drying temperature on dietary fibre, rehydration properties, texture and microstructure of cape gooseberry (*Physalis peruviana* l.). *Journal of Food Science and Technology*, *52*, 2304–2311. https://doi.org/10.1007/s13197-013-1235-0

Wang, C., & Singh, R. (1978). *A single layer drying equation for rough rice*. Retrieved from https://jmie.pure.elsevier.com/en/publications/single-layer-drying-equation-for-rough-rice

Wang, J., Rahman, S., Zhao, X. H., Forghani, F., Park, M. S., & Oh, D. H. (2013). Predictive models for the growth kinetics of *Listeria monocytogenes* on white cabbage. *Journal of Food Safety*, *33*(1), 50–58.

Zhang, M., Chen, H., Mujumdar, A. S., Zhong, Q., & Sun, J. (2015). Recent developments in high-quality drying with energy-saving characteristic for fresh foods. *Drying Technology*, *33*(13), 1590–1600.

How to cite this article: Lopez-Quiroga E, Prosapio V, Fryer PJ, Norton IT, Bakalis S. Model discrimination for drying and rehydration kinetics of freeze-dried tomatoes. *J Food Process Eng*. 2019;e13192. https://doi.org/10.1111/jfpe.13192